THE JOURNAL OF PHYSICAL CHEMISTRY A

Article

Cite This: J. Phys. Chem. A 2018, 122, 1672−1677

pubs.acs.org/JPCA

Combination Rules for Morse-Based van der Waals Force Fields

Li Yang,[†,‡] Lei Sun,[†] and Wei-Qiao Deng*[,†]

[†]State Key Laboratory of Molecular Reaction Dynamics, Dalian National Laboratory for Clean Energy, Dalian Institute of Chemical Physics, Chinese Academy of Sciences, Dalian 116023, China

[‡]University of the Chinese Academy of Sciences, Beijing 100039, China

Supporting Information

ABSTRACT: In traditional force fields (FFs), van der Waals interactions have been usually described by the Lennard-Jones potentials. Conventional combination rules for the parameters of van der Waals (VDW) cross-termed interactions were developed for the Lennard-Jones based FFs. Here, we report that the Morse potentials were a better function to describe VDW interactions calculated by highly precise quantum mechanics methods. A new set of combination rules was developed for Morse-based FFs, in which VDW interactions were described by Morse potentials. The new set of combination rules has been verified by comparing the second virial coefficients of 11 noble gas mixtures. For all of the mixed binaries considered in this work, the combination rules work very well and are superior to all three other existing sets of combination rules reported in the literature. We further used the Morse-based FF by using the combination rules to simulate the adsorption isotherms of CH_4 at 298 K in four covalent-organic frameworks (COFs). The overall agreement is great, which supports the further applications of this new set of combination rules in more realistic simulation systems.

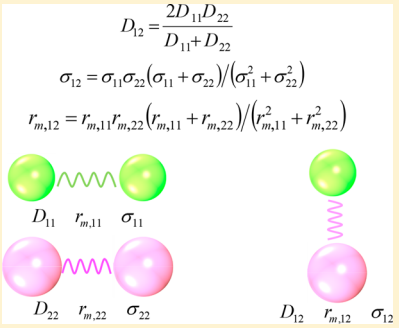

1. INTRODUCTION

Molecular simulation is widely used to predict the properties of systems ranging from biological macromolecules to inorganic compounds. These calculations demand force fields (FFs) describing the intermolecular and intramolecular interactions accurately. Parameters and functional forms are the vital infrastructure of FFs. In most of the popular FFs, the van der Waals (VDW) interactions are often approximated with a Lennard-Jones (LJ 12−6) potential.[1−4] However, the inverse power term ($1/R^{12}$) of LJ 12−6 is known to make the inner wall too stiff. It is noteworthy that there was no effective way to calculate the VDW interaction accurately in the early developed FFs. With the development of computational chemistry, now the VDW interaction can be accurately calculated using ab initio methods such as Møller−Plesset perturbation theory (MP) and coupled cluster with singles and doubles (CCSD) method. On the basis of accurate quantum mechanical (QM) calculations, we find that the Morse potential model reproduces the intermolecular interactions more faithfully than the LJ 12−6 potential. Gambhir and Saxena et al.[5,6] also mentioned that Morse potential was satisfactory in correlating the equilibrium properties of gases and gaseous mixtures and somewhat better than LJ 12−6 and the modified Buckingham Exp-six in interpreting the second virial data of mixtures. Moreover, using an exponential term to represent the repulsive interactions is theoretically more realistic than inverse powers and that the region of true $1/R^6$ character is only at much longer distances. The term of the Morse potential is

$$U_{ij}^{\mathrm{Morse}}(r_{ij}) = D\{\exp[-2C(r^* - r_{\mathrm{m}}^*)] - 2\exp[-C(r^* - r_{\mathrm{m}}^*)]\} \quad (1)$$

where D is the well depth, $r^* = r_{ij}/\sigma$, $r_{\mathrm{m}}^* = r_{\mathrm{m}}/\sigma$, $C = \ln 2/(r_{\mathrm{m}}^* - 1)$, σ is a distance parameter having the physical significance that $U_{ij}^{\mathrm{Morse}}(\sigma_{ij}) = 0$, r_{m} is the well depth position, r_{ij} is the separation of sites i and j, and C is related to the width of the potential well. There is an added flexibility because the Morse potentials have three adjustable parameters instead of two for the LJ 12−6.

The parametrization of the VDW interaction is difficult due to the overabundance of parameters, especially for generic "all-atoms" FFs. Therefore, combining rules are suggested to reduce the parametrization by calculating the unlike pair parameters from the information on like pairs. In most of the popular FFs in use, a geometric mean rule (the Berthelot rule) is used for the energy parameters (like the well depth parameter, D) and a geometric or arithmetic mean rule (the Lorentz rule) for the size parameters (like the well depth position, r_{m}).[1−3] Due to the fact that Lorentz−Berthelot rules can lead to inaccurate mixture properties, numerous other combining rules have been developed. However, most of them are proposed for the LJ potential,[7] while the works developing combination rules for Morse potential are rare.

Three sets of combination rules for the Morse potential were reported to be effective for certain molecular systems.[5,8,9] However, the successes of these rules very much depend on the mixed systems considered. Though the rules of Chang Loyoul Kong[8] are somewhat superior to the other two sets of rules in predicting the second virial coefficients (B_{12}) of Ne−Kr and Ne−Ar mixtures, the complicated forms limit its utilization

Received: November 14, 2017
Revised: January 15, 2018
Published: January 23, 2018

DOI: 10.1021/acs.jpca.7b11252
J. Phys. Chem. A 2018, 122, 1672−1677

in more realistic applications. Thus, proposing a new set of combination rules for the Morse potential, which has a simple form and shows better performance in predicting the mixture properties, is essential.

In this paper, we demonstrate that the Morse potential is superior to LJ 12−6 in approximating the VDW interaction and propose a new set of combination rules for the Morse potential. This new set of combination rules, which requires no new parameters other than D, r_m, and σ, provides excellent fits to the second virial coefficients of noble gas mixtures and shows great performance in predicting the CH_4 uptakes in covalent-organic frameworks (COFs).

2. METHODS

2.1. Combination Rules. A new way to define the forms of combination rules is proposed in this work. We denote the general property of a mixed system A−B by z and the corresponding properties of the pure systems of A−A and B−B by x and y. The function that predicts the value of z from knowledge of x, y is called the combining rule, denoted by $Z(x,y)$. The combining rule must obey three mathematical constraints as Waldman and Hagler[10] proposed.

$$Z(x, y) = Z(y, x) \tag{2}$$

$$Z(x, x) = x \tag{3}$$

$$aZ(x, y) = Z(ax, ay) \tag{4}$$

where a is a constant.

Under the rigorous restriction of these mathematical properties, the two most fundamental functions that obey eqs 2−4 are proposed. One is arithmetic mean rule $Z(x,y) = (x + y)/2$, and another is the geometric mean rule $Z(x,y) = \sqrt{xy}$. Any other candidate functions can be generated by combining these two functions. On the basis of this method, we generated 34 functions as our function library (for more details, see the Supporting Information). On the basis of the function library, we proposed our combination rules by searching the corresponding functional relationship between the unlike and like pair parameters. Parameters were obtained from our prior work.[11] The formula search was performed with a universal global algorithm by the firstOpt software,[12] a leading worldwide software platform for numerical optimization analysis. The formula search results are shown in Table 1. We have considered the physical properties in detail to choose these parameters. The parameter k is the force constant where $r = r_m$. De^{α} represents the repulsive interactions, and $De^{0.5\alpha}$ is the component of the attractive potential. Here, α is a parameter related to C ($\alpha = 2C + 2\ln 2$).

From the results of the formula search, we pick out the candidates that show correlation coefficients larger than 0.5. Consequently, only four parameters are raised: D, r_m, σ, and k.

Considering that the formula search forms for D and k are complicated and the Berthelot rule is known to overestimate the well depth of the parameter significantly, we suggest to use the harmonic mean (eq 5) with a correlation coefficient of 0.606, which is not significantly smaller than the largest one (0.644) in the formula search for D.

$$D_{12} = \frac{2D_{11}D_{22}}{D_{11} + D_{22}} \tag{5}$$

For the rules for r_m and σ, we use the formula search results in eqs 6 and 7.

Table 1. Maximum Correlation Coefficients and the Terms of the Combination Rules in the Formula Search

parameter	function	R_{max}
D	$z = 2Z_1Z_4/(Z_1 + Z_4)$	0.644
r_m	$z = xy(x + y)/(x^2 + y^2)$	0.621
α	$z = xy(x + y)/(x^2 + y^2)$	0.180
σ	$z = xy(x + y)/(x^2 + y^2)$	0.558
C	$z = xy(x + y)/(x^2 + y^2)$	0.186
r_m/α	$z = ((x^6 + y^6)/2)^{1/6}$	0.160
α/r_m	$z = (x + y)^2/(4(xy)^{1.5})$	0.058
k	$z = 2Z_1Z_4/(Z_1 + Z_4)$	0.623
De^{α}	$z = 2Z_1Z_4/(Z_1 + Z_4)$	0.376
$De^{0.5\alpha}$	$z = \sqrt{Z_1Z_4}$	0.465

$$\sigma_{12} = \sigma_{11}\sigma_{22}(\sigma_{11} + \sigma_{22})/(\sigma_{11}^2 + \sigma_{22}^2) \tag{6}$$

$$r_{m,12} = r_{m,11}r_{m,22}(r_{m,11} + r_{m,22})/(r_{m,11}^2 + r_{m,22}^2) \tag{7}$$

2.2. Second Virial Coefficients. The algorithms of the second virial coefficient for the Morse potential are given by Konowalow et al.[13] Morse potential parameters determined from the second virial coefficient for pure gas are given in Table S1 (Supporting Information). The values of the reduced virial coefficients are tabulated in ref 13 as a function of C, T^*, and r_m^*. All of the experimental B_{12} values obtained from ref 14 are calculated under the equal mole fraction ($X_1 = X_2$).

2.3. Parameterization Procedure. Ab initio configuration interaction calculations have been carried out for two clusters (He−He and Ar−Ar) to provide a numerical test of the Morse potential and LJ 12−6 potential. Geometry optimizations and single-point energy calculations were at the CCSD(T)/aug-cc-pv5z level. All binding energies in the binary systems were corrected using basis set superposition error (BSSE) by the full counterpoise procedure. During the numerical fitting, parameters D and r_m were extrapolated directly from the ab inito calculations. For fitting results, see Table 2.

Table 2. Potential Parameters for He−He and Ar−Ar

	Morse			LJ 12−6	
gas	D (kJ/mol)	r_m (Å)	α	D (kJ/mol)	r_m (Å)
He−He	0.08185	2.9908	12.663	0.08185	2.9908
Ar−Ar	1.09091	3.8000	12.640	1.09091	3.8000

Geometry optimizations of CH_4−CH_4 N2−N2 and H2−H2 were under the CCSD(T) level, while MP2 was used for other binary systems: C_6H_6−C_6H_6, $B_3O_3H_3$−$B_3O_3H_3$, $Si(CH_3)_4$−$Si(CH_3)_4$. We used a quadruple-ζ valence basis (QZV) supplemented with polarization functions from the cc-PVTZ basis denoted as QZVPP. All binding energies in the binary systems were corrected using BSSE by the full counterpoise procedure. QM calculations were performed using the Gaussian 09 code.[15] We considered four different geometrical configurations for CH_4−CH_4, C_6H_6−C_6H_6, $Si(CH_3)_4$−$Si(CH_3)_4$, and $B_3O_3H_3$−$B_3O_3H_3$ dimers, respectively, which are shown in Figure 1.

For C_6H_6−C_6H_6 and $B_3O_3H_3$−$B_3O_3H_3$ dimers, the distance between two monomers is characterized by the distance between

DOI: 10.1021/acs.jpca.7b11252
J. Phys. Chem. A 2018, 122, 1672−1677

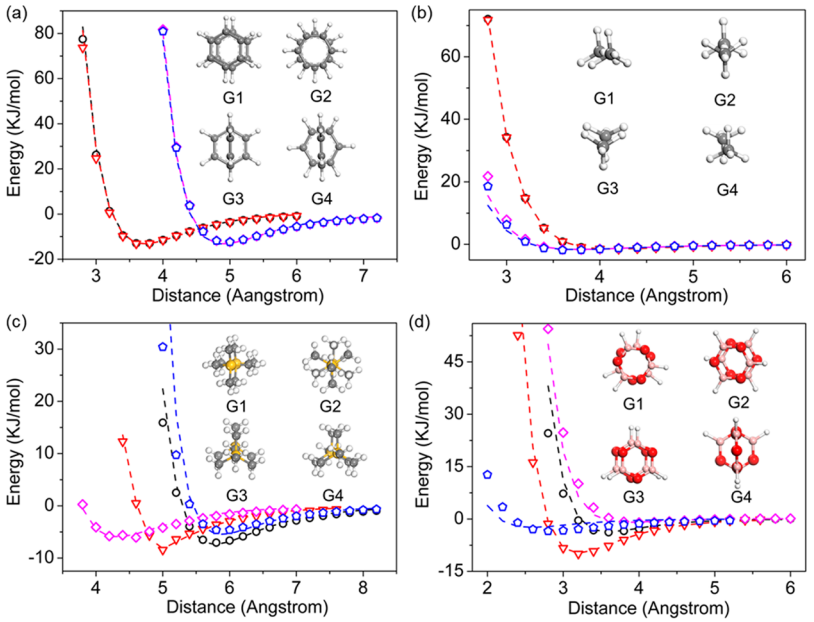

Figure 1. Comparison of the fitted FF energies with QM results: (a) C_6H_6−C_6H_6, (b) CH_4−CH_4, (c) $Si(CH_3)_4$−$Si(CH_3)_4$, (d) $B_3O_3H_3$−$B_3O_3H_3$. Intermolecular interaction energies for a CH_4 dimer were calculated at the CCSD(T)/QZVPP level, while energies for other dimers were calculated at the MP2/QZVPP level. Here C atoms are brown, B pink, O red, Si yellow, and H white. FF results are shown as dashed lines, while the QM results are shown by empty symbols. Black: G1; red: G2; magenta: G3; blue: G4.

the center of mass. However, for CH_4−CH_4 and $Si(CH_3)_4$−$Si(CH_3)_4$, the distance is the separation between C−C or Si−Si. The FF types in each molecular cluster are listed in Table S4. Our new parameters are shown in Tables S5 and S6. Table S5 shows the parameters of like pairs obtained from fitting QM calculations, while the parameters of unlike pairs were directly calculated using the combination rules shown in Table S6.

2.4. GCMC Procedure. The covalent bonds of the framework for COFs and CH_4 were treated by a generic FF, Universal FF (UFF), which was accurate for predicting the structure of COFs. These simulations used two 2D-COFs (COF-5,[16] COF-10[17]) and two 3D-COFs (COF-102,[18] COF-103[18]). The physical properties of the frameworks are summarized in Table S7. Before the simulation, we had optimized the structures of the four COFs. The optimizations were performed by the DMol3 package[19−22] based on density functional theory (DFT) using a PBE (Perdew, Burke, and Enzerhof) functional and a double-numeric quality basis set with polarization functions (DND). For the structures of COF-5 and COF-10, we used 1 × 1 × 5 and 1 × 1 × 4 supercells, respectively, while unit cells were used for the other two 3D-COFs. Atomic charges of the frameworks and methane arose from the Mulliken population analysis. Framework charges were obtained from the DFT calculations, while those of methane were determined by the ab initio methods. To determine the gas storage capacity, the grand canonical Monte Carlo method was used. We assigned each atom with an atomic FF type, as shown in Table S4. To obtain an accurate measure of the molecular loading, we ran 10 000 000 equilibration steps before the production stage and 10 000 000 Monte Carlo steps in the production stage. We also computed the density of gas-phase methane at 273, 298, and 323 K by performing the GCMC simulations. There is good agreement between our combination rule-based simulation results and experimental data from the National Institute of Standards and Technology (NIST). See Figure 2.

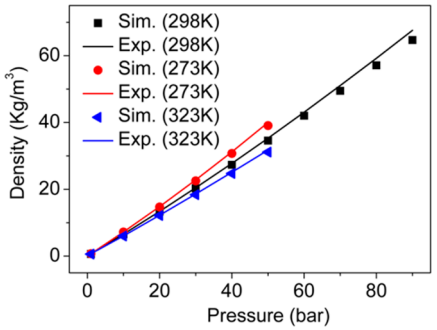

Figure 2. Methane density calculated from theory and experiment at different temperatures (273, 298, 323 K) as a function of pressure.

3. RESULTS AND DISCUSSION

3.1. Numerical Test of the Morse Potential and LJ 12−6 Potential. It is known that the parameter α makes the Morse potential more flexible than LJ 12−6. Moreover, the inverse power term $(1/R^{12})$ of the repulsive potential makes the inner wall too stiff. As shown in Figure 3, the Morse potential

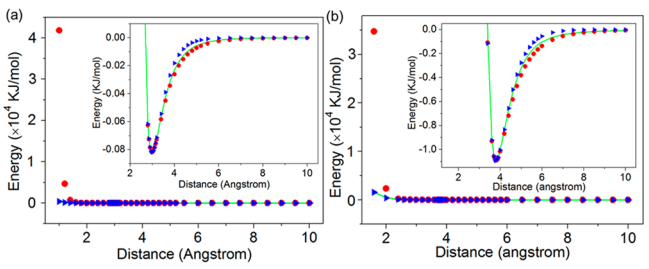

Figure 3. Comparison of the fitted FF (point) and QM (line) energies for two systems: (a) He−He; (b) Ar−Ar. circle: LJ potential; triangle: Morse potential. The insets show the accuracy in fitting to the equilibrium distance.

DOI: 10.1021/acs.jpca.7b11252
J. Phys. Chem. A 2018, 122, 1672−1677

Table 3. Combining Rules for Morse Potential Parameters

	combining rules[a]
Saxena and Gambhir[5]	$D_{12} = \sqrt{D_{11}D_{22}}$ (i)
	$\frac{C_{12}}{\sigma_{12}} = \frac{1}{2}\left(\frac{C_{11}}{\sigma_{11}} + \frac{C_{22}}{\sigma_{22}}\right)$ (ii)
	$\sigma_{12} = 2C_{12}\left[\frac{C_{11}}{\sigma_{11}} + \frac{C_{22}}{\sigma_{2}}\right]^{-1}$ (iii)
Saran[9]	eq i
	eq ii
	$\sigma_{12} = \sqrt{\sigma_{11}\sigma_{22}}$ (iv)
Chang Lyoul Kong[8]	$\left[\frac{D_{12}C_{12}}{\sigma_{12}}e^{2C_{12}}\right]^{\sigma_{12}/C_{12}} = \left[\frac{D_{11}C_{11}}{\sigma_{11}}e^{2C_{11}}\right]^{\sigma_{11}/2C_{11}}\left[\frac{D_{22}C_{22}}{\sigma_{22}}e^{2C_{11}}\right]^{\sigma_{22}/2C_{22}}$ (v)
	$\frac{\sigma_{12}}{C_{12}} = \frac{1}{2}\left[\frac{\sigma_{11}}{C_{11}} + \frac{\sigma_{22}}{C_{22}}\right]$ (vi)
	$D_{12}e^{\sigma_{12}(C_{11}/2\sigma_{11}+C_{22}/2\sigma_{22})} = \sqrt{D_{11}e^{C_{11}}D_{22}e^{C_{22}}}$ (vii)
new rules	eqs 5−7

[a]The subscripts 11, 22, and 12 denote the like sites pair and unlike sites pair.

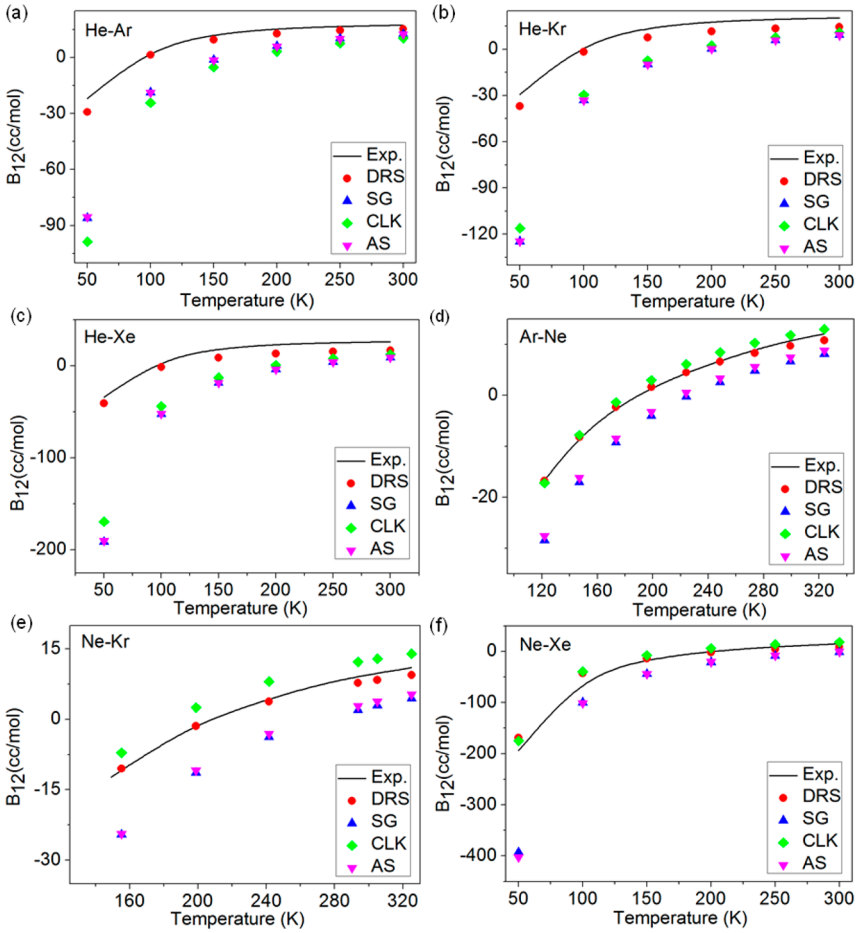

Figure 4. Comparison of experimental and calculated second virial coefficients B_{12} of noble gas mixtures. Calculated (symbols): circle, our work (DRS); triangle up, Saxena-Gambhir's rules (SG); rhombus, Chang Lyoul Kong's rules (CLK); triangle down, Saran's rules (AS). The black line is experimental data: (a−f);[14] (d,e).[23]

reproduces the QM results of He−He and Ar−Ar dimers better than the LJ 12−6 potential, especially in the repulsive region. The $1/R^{12}$ term in LJ 12−6 approximates the repulsion rather poorly. Although it is generally considered that the conformations near the potential well are more important, the repulsive part will play a major role under high pressure. Our prior work[11] has tested the

DOI: 10.1021/acs.jpca.7b11252
J. Phys. Chem. A 2018, 122, 1672−1677

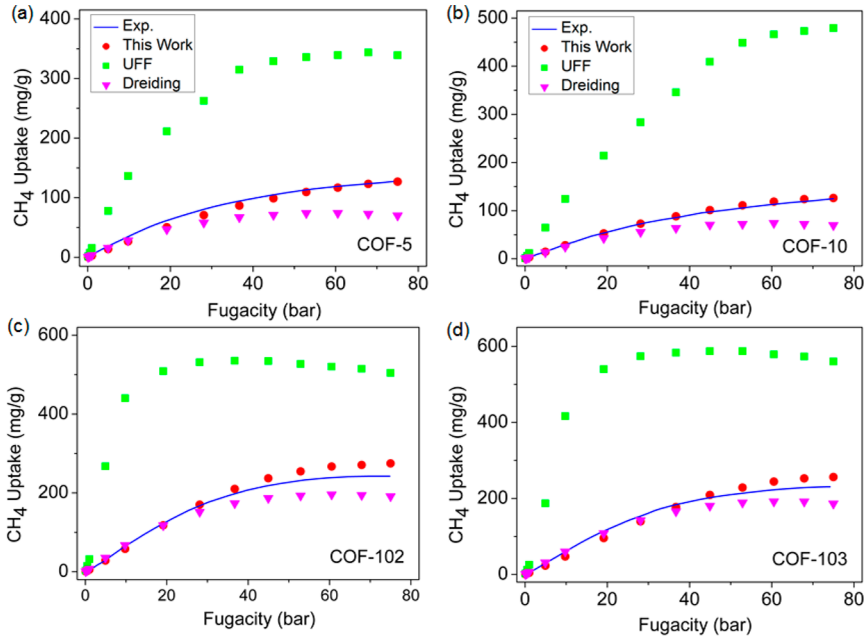

Figure 5. Excess methane adsorption isotherms at 298 K: (a) COF-5; (b) COF-10; (c) COF-102; (d) COF-103. Symbol codes: solid line (experiment), square (Universal), triangle (Dreiding), circle (this work).

performances of Pcff, UFF, Dreiding, and Compass FFs in predicting gas densities of CH_4, CO_2, and N_2. None of the popular used FFs predicts the gas densities correctly at high pressure. This may be just due to the fact that LJ 12−6 does not describe the repulsive interactions reasonably. Thus, we believe that it is more accurate to approximate the complicated VDW interaction with the Morse potential.

3.2. Test Combination Rules by Comparing Calculated and Experimental Second Virial Coefficients of Noble Gas Mixtures. To have a comparative test on our new rules and other combination rules suggested for the Morse potential previously (see Table 3), the computed mixed second virial coefficients B_{12} of 11 mixtures employing the unlike pair parameters predicted by each set of the combining rules were compared with experimental measurements.

Eleven mixtures are He−Ne, He−Ar, He−Kr, He−Xe, Ne−Ar, Ne−Kr, Ne−Xe, Ar−Kr, Ar−Xe, Kr−Xe, and Ar−CH_4. Comparison of experimental[14,23,24] and calculated second virial coefficients B_{12} of six noble gas mixtures are shown in Figure 4; those for the other five mixtures can be found in Figure S1.

For He−Ar, He−Kr, and He−Xe mixtures, our new rules are clearly superior to the other three sets of rules (see Figure 4a−c). For Ne−Ar, Ne−Kr, Ne−Xe, and Ar−Xe mixtures, our work and the rules of Chang Lyoul Kong show the same nature, while the other two sets of rules have significant deviation from the experimental values (see Figures 4d−f and Figure S1d). All sets of combining rules work very well in the Ar−Kr, Kr−Xe, and Ar−CH_4 mixtures (see Figure S1c,b,e). Though four sets of rules have discrepancies between computing and experimental values in the He−Ne mixture (see Figure S1a), our combination rules are somewhat superior to the other three sets of combination rules. It seems to be that the successes of the other three sets of rules are very much mixed depending on the system considered. While our new set of rules works without any single case of serious failure for all of the mixtures considered here. It has been pointed out in previous works[8,25] that most of the combining rules give the same unlike pair parameters for systems with the closer like pair parameters, but even the best of the previous rules fails to predict proper unlike pair parameters for systems such as He−Ar and He−Xe involving molecules with a large difference in the "size" of like pairs.

Considering that all of the tests above investigate only the B_{12} at lower temperatures, we calculate B_{12} for six mixtures (N_2−H_2, N_2−He, He−H_2, He−Ne, Ar−H_2, Ar−He) at higher temperatures. The results are listed in Table S2. Four sets of combining rules have no significant difference among one other in B_{12} of the six mixtures at higher temperatures.

3.3. Comparison between Theoretical and Experimental Methane Adsorption Isotherms of Four COFs. To further evaluate the performance of our rules in more realistic applications, such as simulation of gas adsorption, our new set of rules was used to develop the VDW FF parameters. To validate the FF parameters based on our new rule, we simulated the methane storage capacity in four COFs using the GCMC method with the FF parameters and compared the simulated uptakes with the experimental values of Hiroyasu Furukawa and Omar M. Yaghi.[26]

In Figure 5, we compare the excess methane adsorption isotherms at 298 K from simulations to experiments.[26] The simulated adsorption isotherms of COF-5 and COF-10 agree well with the reported experimental data at both low- and high-pressure conditions. The predicted excess methane uptake in COF-5 is 124 mg/g at 85 bar, in excellent agreement with the experimental value of 127 mg/g. Similarly, the predicted excess uptake of 126 mg/g in COF-10 at 85 bar is close to the experimental result of 124 mg/g. For COF-102 and COF-103, our simulations show a small positive deviation in the high-pressure region. However, the deviation is negligible, and the overall agreement is good. Obviously, the UFF overestimates the excess uptake of CH_4 in four COFs, while the result of Dreiding is a bit of an understatement. Our new VDW parameters perform better than both UFF and Dreiding. These results suggest that our FF parameters developed by using our new combination rules provide a good estimation of the COF−methane interaction at 298 K. It is further suggested that our combination rules are credible to be used to generate unlike pair parameters.

DOI: 10.1021/acs.jpca.7b11252
J. Phys. Chem. A 2018, 122, 1672−1677

4. CONCLUSIONS

We illustrated that the Morse potential is somewhat superior to LJ 12−6 in approximating the VDW interactions and proposed a new set of combination rules for the Morse potential. We used the second virial coefficients of 11 binary mixtures to test our combining rules and three sets of combination rules reported in the literature. It has been shown that our new rules work without any single case of serious failure in the above mixed systems and are superior to the other three sets of combination rules. The GCMC simulations with the FF parameters developed by combining our new rules with fitting QM results show a good agreement between theory and experiment for CH_4 excess uptakes in four COFs. In our future work, we will establish an accurate VDW FF with the combination rules for gas adsorption in porous materials.

■ ASSOCIATED CONTENT

Supporting Information

The Supporting Information is available free of charge on the ACS Publications website at DOI: 10.1021/acs.jpca.7b11252.

Process of proposing combination rules; methodology and pure gaseous Morse potential parameters for computing mixed second virial coefficients; comparison of experimental and calculated second virial coefficients B_{12} of noble gas mixtures at higher temperatures; comparison of our fit with the standard approach in H_2 and N_2 systems; experimental and calculated second viral parameters at higher temperatures; force field type in each molecular cluster; like and unlike pair parameters in fitting results; and structural characteristics of covalent-organic frameworks investigated in this work (PDF)

■ AUTHOR INFORMATION

Corresponding Author

*E-mail: dengwq@dicp.ac.cn.

ORCID

Wei-Qiao Deng: 0000-0002-3671-5951

Notes

The authors declare no competing financial interest.

■ ACKNOWLEDGMENTS

This work was supported by the National Key Research and Development Program of China (No. 2017YFA0204800), the National Science and Technology Major Project of the Ministry of Science and Technology of China (No. 2017ZX05036001), the Chinese Academy of Sciences (No. XDB10020201), and the National Natural Science Foundation of China (No. 21525315, 21403211, and 91333116).

■ REFERENCES

(1) Rappé, A. K.; Casewit, C. J.; Colwell, K. S.; Goddard, W. A., III; Skiff, W. M. UFF, a Full Periodic Table Force Field for Molecular Mechanics and Molecular Dynamics Simulations. *J. Am. Chem. Soc.* **1992**, *114*, 10024−10035.

(2) Mayo, S. L.; Olafson, B. D.; Goddard, W. A., III DREIDING: A Generic Force Field for Molecular Simulations. *J. Phys. Chem.* **1990**, *94*, 8897−8909.

(3) Hagler, A. T.; Huler, E.; Lifson, S. Energy Functions for Peptides and Proteins. I. Derivation of a Consistent Force Field Including the Hydrogen Bond from Amide Crystals. *J. Am. Chem. Soc.* **1974**, *96*, 5319−5327.

(4) Cornell, W. D.; Cieplak, P.; Bayly, C. I.; Gould, I. R.; Merz, K. M.; Ferguson, D. M.; Spellmeyer, D. C.; Fox, T.; Caldwell, J. W.; Kollman, P. A. A Second Generation Force Field for the Simulation of Proteins, Nucleic Acids, and Organic Molecules. *J. Am. Chem. Soc.* **1995**, *117*, 5179−5197.

(5) Saxena, S. C.; Gambhir, R. S. Second Virial Coefficient of Gases and Gaseous Mixtures on the Morse Potential. *Mol. Phys.* **1963**, *6*, 577−583.

(6) Gambhir, R. S.; Saxena, S. C. Zero Pressure Joule-Thomson Coefficient for a Few Non-Polar Gases on the Morse Potential. *Indian J. Phys.* **1963**, *37*, 540−2.

(7) Schnabel, T.; Vrabec, J.; Hasse, H. Unlike Lennard−Jones Parameters for Vapor−Liquid Equilibria. *J. Mol. Liq.* **2007**, *135*, 170−178.

(8) Kong, C. L. Combining Rules for Intermolecular Potential Parameters. II. Rules for the Lennard-Jones (12−6) Potential and the Morse Potential. *J. Chem. Phys.* **1973**, *59*, 2464−2467.

(9) Saran, A. Potential Parameters for Like and Unlike Interactions on Morse Potential Model. *Indian J. Phys.* **1963**, *37*, 491−499.

(10) Waldman, M.; Hagler, A. T. New Combining Rules for Rare Gas van der Waals Parameters. *J. Comput. Chem.* **1993**, *14*, 1077−1084.

(11) Sun, L.; Yang, L.; Zhang, Y. D.; Shi, Q.; Lu, R. F.; Deng, W. Q. Accurate van der Waals Force Field for Gas Adsorption in Porous Materials. *J. Comput. Chem.* **2017**, *38*, 1991−1999.

(12) 7D-Soft High Technology Inc. *1stOpt manual*, release 7.0. http://www.7d-soft.com/ (Accessed April 20, 2016).

(13) Konowalow, D. D.; Taylor, M. H.; Hirschfelder, J. O. Second Virial Coefficient for the Morse Potential. *Phys. Fluids* **1961**, *4*, 622.

(14) Kestin, J.; Knierim, K.; Mason, E. A.; Najafi, B.; Ro, S. T.; Waldman, M. Equilibrium and Transport Properties of the Noble Gases and Their Mixtures at Low Density. *J. Phys. Chem. Ref. Data* **1984**, *13*, 229−303.

(15) Frisch, M. J.; Trucks, G. W.; Schlegel, H. B.; Scuseria, G. E.; Robb, M. A.; Cheeseman, J. R.; Montgomery, J. A.; Vreven, T.; Kudin, K. N.; Burant, J. C.; et al. *Gaussian 09*, revision C.01; Gaussian, Inc.: Wallingford, CT, 2009.

(16) Cote, A. P.; Benin, A. I.; Ockwig, N. W.; O'Keeffe, M.; Matzger, A. J.; Yaghi, O. M. Porous, Crystalline, Covalent Organic Frameworks. *Science* **2005**, *310*, 1166−1170.

(17) Cote, A. P.; El-Kaderi, H. M.; Furukawa, H.; Hunt, J. R.; Yaghi, O. M. Reticular Synthesis of Microporous and Mesoporous 2D Covalent Organic Frameworks. *J. Am. Chem. Soc.* **2007**, *129*, 12914−12915.

(18) El-Kaderi, H. M.; Hunt, J. R.; Mendoza-Cortés, J. L.; Côté, A. P.; Taylor, R. E.; O'Keeffe, M.; Yaghi, O. M. Designed Synthesis of 3D Covalent Organic Frameworks. *Science* **2007**, *316*, 268−272.

(19) Kessi, A.; Delley, B. Density Functional Crystal vs. Cluster Models as Applied to Zeolites. *Int. J. Quantum Chem.* **1998**, *68*, 135−144 (DMol3 code)..

(20) Delley, B. An All-Electron Numerical Method for Solving the Local Density Functional for Polyatomic Molecules. *J. Chem. Phys.* **1990**, *92*, 508−517.

(21) Delley, B. A Scattering Theoretic Approach to Scalar Relativistic Corrections on Bonding. *Int. J. Quantum Chem.* **1998**, *69*, 423−433.

(22) Delley, B. From Molecules to Solids With the $DMol^3$ Approach. *J. Chem. Phys.* **2000**, *113*, 7756−7764.

(23) Brewer, J. *Determination of Mixed Virial Coefficients*; Air Force Office of Scientific Research, 1967; pp 67−2795.

(24) Thomaes, G.; van Steenwinkel, R.; Stone, W. The Second Virial Coefficient of Two Gas Mixtures. *Mol. Phys.* **1962**, *5*, 301−306.

(25) Lin, H.-M.; Robinson, R. L. Test of Combination Rules for Prediction of Interaction Second Virial Coefficients. *J. Chem. Phys.* **1971**, *54*, 52−58.

(26) Furukawa, H.; Yaghi, O. M. Storage of Hydrogen, Methane, and Carbon Dioxide in Highly Porous Covalent Organic Frameworks for Clean Energy Applications. *J. Am. Chem. Soc.* **2009**, *131*, 8875−8883.

DOI: 10.1021/acs.jpca.7b11252
J. Phys. Chem. A 2018, 122, 1672−1677